Adaptive Optics Simulation of Intraocular Lenses with Modified Spherical Aberration

Patricia A. Piers,[1] *Enrique J. Fernandez,*[2] *Silvestre Manzanera,*[2] *Sverker Norrby,*[1] *and Pablo Artal*[2]

Purpose. Adaptive optics systems can be used to investigate the potential visual benefit associated with correcting ocular wave-front aberration. In this study, adaptive optics techniques were used to evaluate the potential advantages and disadvantages associated with intraocular lenses (IOLs) with modified spherical aberration profiles.

Methods. An adaptive optics vision simulator was constructed that allows psychophysical tests to be performed while viewing targets through any desired ocular wave-front profile. With this simulator, the subjective visual performance of four subjects was assessed by letter acuity and contrast sensitivity (at 3, 6, and 15 cyc/deg) for two different values of induced spherical aberration. The values of spherical aberration were chosen to reproduce two conditions: the average amount measured in pseudophakic patients with implanted IOLs having spherical surfaces and the complete correction of the individual's spherical aberration. Visual performance was assessed in both white and green light, at best focus and for defocus of ± 0.5 and ± 1.0 D.

Results. There was an average improvement in visual acuity associated with the correction of spherical aberration of 10% and 38% measured in white and green light, respectively. Similarly, average contrast sensitivity measurements improved 32% and 57% in white and green light. When spherical aberration was corrected, visual performance was as good as or better than for the normal spherical aberration case for defocus as large as ± 1 D.

Conclusions. Correcting ocular spherical aberration improves spatial vision in the best-focus position without compromising the subjective tolerance to defocus. (*Invest Ophthalmol Vis Sci.* 2004;45:4601–4610) DOI:10.1167/iovs.04-0234

The unique wave-front aberration profile of an individual eye[1,2] is an important factor in defining the visual performance that is achieved with that eye. A reduction in wave-front aberration improves ocular optical quality, the contrast of images formed on the retina, and thus spatial vision.[3–8] In recent times, much attention in the fields of vision science and ophthalmology has been paid to improving visual performance by reducing higher-order ocular wave-front aberrations (those beyond astigmatism and defocus). Guirao et al.[9] calculated the contrast improvement expected if higher-order aberrations were to be corrected in a large population of eyes and discovered that some people would experience very small improvements, whereas others would appreciate significant improvements. With visual enhancement as the ultimate goal, several techniques have been used both in the laboratory—adaptive optics[4,7,10–13] and phase plates[14]—and in the clinical environment—customized corneal refractive surgery,[5,15,16] customized contact lenses,[17] and IOLs.[8,18–20]

Vision research has been expanded appreciably through the use of adaptive optics in recent years. Liang et al.[4] used adaptive optics to correct higher-order aberration, with resultant improved contrast sensitivity. Yoon and Williams[7] conducted more in-depth experiments to study the impact on visual performance of the correction of the wave-front aberration with adaptive optics. They extended measurements to include monochromatic and polychromatic contrast sensitivity and visual acuity testing and found improvements in the contrast sensitivity (at 16 and 24 cyc/deg) on the order of two times in polychromatic light and on the order of three times in monochromatic light. More recently, Fernandez et al.[13] used adaptive optics to investigate the impact of different aberration patterns on letter acuity and found that even when a subject's wave-front aberration is altered in a manner that results in similar modulation transfer functions (MTFs) and root mean squared (RMS) wave-front aberration errors, visual acuity could be surprisingly different. These results demonstrate that adaptive optics is a powerful tool for a controlled laboratory study of the visual benefit of correcting higher-order aberrations.

IOLs are a natural candidate for practical static correction of higher order aberrations. The Tecnis IOL (AMO, Santa Ana, CA) attempts partial correction of the wave-front aberration by removing spherical aberration. It was designed with aspheric optics, to correct the average corneal spherical aberration of an average patient with cataract.[21] Recent studies have revealed that this lens successfully eliminates spherical aberration in the average pseudophakic eye.[8] The average postoperative Zernike coefficient for spherical aberration ($Z(4,0)$) for a 4-mm pupil was 0.007 μm in eyes with Tecnis IOL implants and 0.081 μm in eyes with spherically surfaced IOL implants (SI40NB; AMO). These results showed that when currently available spherically surfaced IOLs are implanted, significant amounts of positive spherical aberration remain uncorrected. As a result of the correction provided by the Tecnis lens, the postoperative contrast vision of patients was improved.[8,19,20] At present, this is the only IOL that attempts to reduce the postoperative wave-front aberration of pseudophakic eyes. However, it corrects for the average corneal spherical aberration. It is therefore unclear what the visual benefit would be with either a customized IOL designed to correct all wave-front aberrations or an aspheric lens customized for the individual and designed to

From [1]AMO Groningen, Groningen, The Netherlands; and [2]Laboratorio de Optica, Departamento de Fisica, Universidad de Murcia, Murcia, Spain.

Presented in part at the annual meeting of the Association for Research in Vision and Ophthalmology, Fort Lauderdale, Florida, May 2003.

Supported by AMO Groningen and Grant BFM2001-0391 from Ministerio de Ciencia y Tecnología, Spain.

Submitted for publication March 2, 2004; revised June 17, 2004; accepted June 21, 2004.

Disclosure: **P.A. Piers**, AMO (E, P); **E.J. Fernandez**, AMO (C); **S. Manzanera**, AMO (C); **S. Norrby**, AMO (E, P); **P. Artal**, AMO (C, P)

The publication costs of this article were defrayed in part by page charge payment. This article must therefore be marked "*advertisement*" in accordance with 18 U.S.C. §1734 solely to indicate this fact.

Corresponding author: Patricia A. Piers, AMO Groningen, P.O. Box 901, 9700 AX Groningen, The Netherlands; patricia.piers@amo-inc.com.

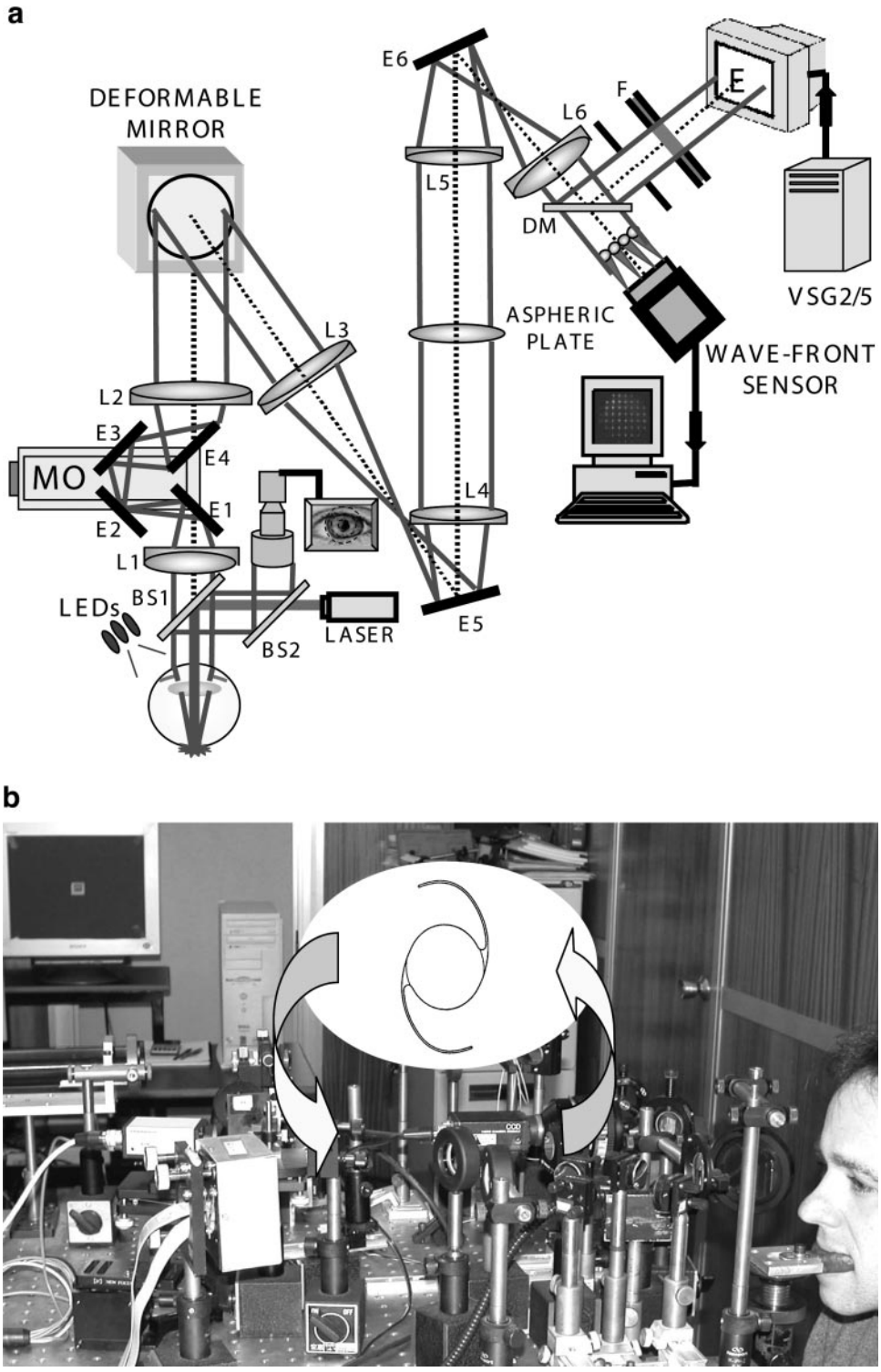

FIGURE 1. (**a**) Diagram of the AOVS. (**b**) The actual experimental system that reproduces the optical properties of a customized IOL.

completely correct the spherical aberration. Along with the potential benefits, it has also been suggested that ocular spherical aberration increases depth of focus and therefore increases tolerance to defocus.[22,23]

To investigate both the potential advantages and disadvantages of new theoretical designs of IOLs, an adaptive optics vision simulator (AOVS) employing a membrane deformable mirror has been developed at the University of Murcia.[24] In this study, we used this system to investigate the potential of IOLs that provide customized correction of spherical aberration (correct the spherical aberration for each individual's eye). We also investigated how this correction would affect subjective tolerance to defocus. Measurements of visual acuity and contrast sensitivity were performed to determine whether an IOL that perfectly corrects both refractive error (defocus and astigmatism) and spherical aberration would have a measurable positive impact on visual performance. Measurements were performed in both monochromatic and polychromatic light to evaluate the role of chromatic aberration.

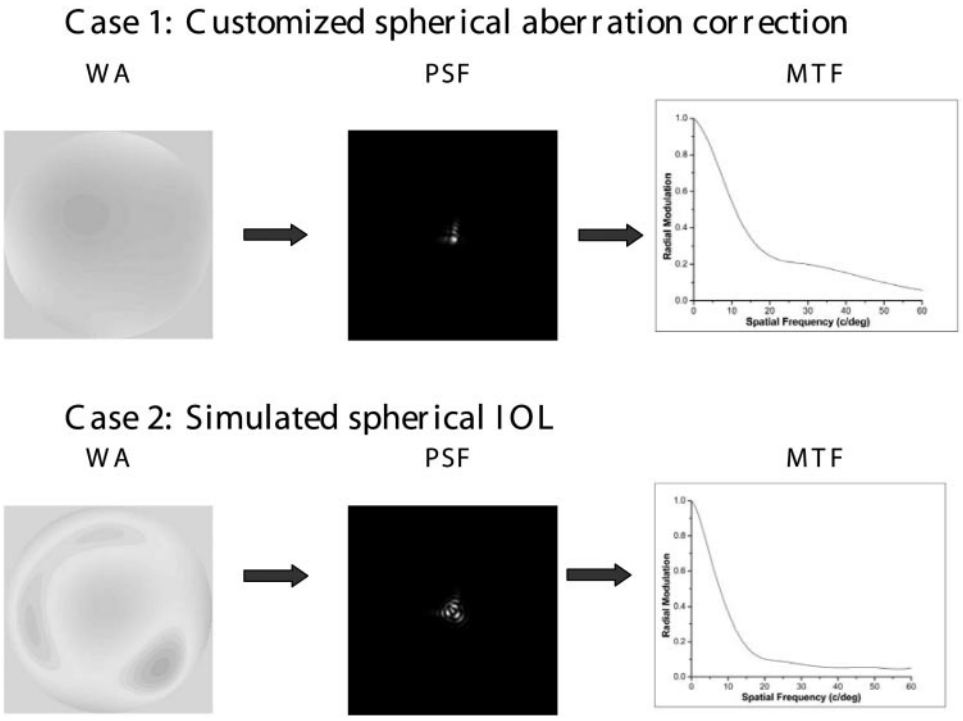

FIGURE 2. The measured wave-front aberration (WA), PSF, and MTF for subject EV with (**a**) spherical aberration corrected (case 1) and (**b**) 0.149 μm of spherical aberration introduced for a 4.8-mm pupil (case 2).

METHODS

Apparatus: Adaptive Optics Visual Simulator

Figure 1a shows a schematic diagram of the AOVS apparatus. A near-infrared (780 nm) diode laser is used for illuminating the eye after reflection from a beam splitter (BS1). The eye's pupil is optically conjugated by means of lenses (achromatic doublets L1 and L2) with the membrane deformable mirror. Additional lenses (achromatic doublets L3–L6) also conjugate the eye's pupil with a Hartmann-Shack wave-front sensor,[1,25] which is used to measure the ocular aberrations. A motorized, computer-controlled optometer, a set of four mirrors (E1–E4), mounted on a translation stage (MO) is used either to correct or to induce defocus. A dichroic mirror (DM), placed after lens L6 and before the wave-front sensor, allows the subject to see an object (e.g., letter chart, grating) with any desired modified aberration pattern. The insertion or removal of an interference filter (F) permits visual testing either in monochromatic or white light.

The membrane deformable mirror[26] has 37 electrodes under the metallic membrane. It works by electrostatic forces (i.e., voltages applied independently to each electrode induce the required local shape of the membrane). To control the deformable mirror, the membrane's influence functions are first measured. These are the functions that describe the shape of the mirror membrane when a given voltage is applied to each particular electrode. Assuming that the membrane deformation follows a linear superposition of these influence functions, it is straightforward to obtain the required set of voltages to produce a desired mirror shape. This is an iterative process controlled by the continuous measurement of the mirror's shape by the real-time wave-front sensor. The complete process to produce a desired shape in the mirror requires approximately five iterations, corresponding to ~0.2 seconds. Additional details concerning the calibration and testing of this type of deformable mirror can be found elsewhere.[24]

Once the aberrations have been modified, a second channel is used for testing the subject's visual quality. The targets used for these vision tests are displayed using a high-resolution monitor and a visual stimulus generator (VSG2/5; Cambridge Research Systems, Rochester, UK). This system, placed in the visual path of the subject provides the simulator with the ability to perform sophisticated psychophysical testing.

The range of defocus that can be induced is quite large (generated with the motorized optometer). However, the maximum amount of higher-order aberration modes that can be produced is approximately 0.5 μm. The actual limit depends on the mode and is lower for spherical aberrations. For this reason, spherical aberration was corrected or introduced by placing aspheric phase plates with different amounts of spherical aberration in the setup at a plane conjugate with the subject's pupil (by lenses L1–L4). The AOVS requires precise alignment of the subject's pupil with both the membrane mirror and the wave-front sensor. This is achieved by stabilizing the subject's head with a bite bar and monitoring the pupil position with a video camera through beam splitters BS1 and BS2 when the front of the eye is illuminated with a set of infrared LEDs. The system is robust enough to accommodate blinking, which ensures the simulator's usefulness for long-duration visual testing.

Subjective visual testing was performed using both polychromatic (white) and green targets. Green targets were created by viewing the polychromatic targets through a narrow-band interference filter cen-

TABLE 1. Spherical Aberration Measured in Each Subject Throughout the Duration of the Experiment

	EV		JF		PP		SM	
	1*	2	1	2	1	2	1	2
Mean spherical aberration	−0.0052	0.1685	0.0038	0.1382	−0.0011	0.1625	0.0048	0.1447
Standard deviation	0.0101	0.0062	0.0096	0.0079	0.0158	0.0152	0.0075	0.0075

* Data represent cases 1 and 2.

tered on 540 nm. Because the wave-front aberrations and the defocus of the subject were measured in infrared light, the optometer was positioned so as to take into account the difference in focus between the green and infrared light brought about by longitudinal chromatic aberration. The luminance at the eye measured for the white light viewing condition was 35 cd/m^2, whereas the luminance measured for the green light condition was 24 cd/m^2. Although both luminance levels were in the photopic range, the fact that the white and green luminances were different means that no direct comparison of these measurements can be made.

Figure 1b shows an actual picture of the AOVS apparatus. The complete set of optical elements serves to simulate precisely the effect of an IOL with a desired aberration profile (as schematically indicated in the figure).

Subjects and Experimental Conditions

The experiment was performed in four normal young subjects (JF, PP, SM, and EV) aged 27, 29, 31, and 29, respectively. The subjects were all white and were selected after passing a complete ophthalmic examination. The study adhered to the tenets of the Declaration of Helsinki, and signed informed consent was obtained from every subject after the nature and all possible consequences of the study had been explained. Measurements of subjective visual quality were performed in both green light and white light for a 4.8-mm (artificial) pupil size. Two drops of 1% tropicamide were instilled approximately 0.5 hour before the experiments, to initiate cycloplegia and mydriasis.

Subjective measurements of visual performance (acuity and contrast sensitivity) were then obtained for two cases.

Case 1. The spherical aberration of the subject's eye was corrected with a combination of phase plates and the deformable mirror. All other higher-order wave-front aberrations present in the subjects' eyes remained unmodified.

Case 2. After introducing the spherical aberration typically measured in a pseudophakic population with spherical IOL implants ($Z(4,0) = 0.149$ μm for a 4.8-mm pupil) in the subject's eye. This value was based on the spherical aberration measured in the pseudophakic population studied by Mester et al.[8] and from the corneal spherical aberration found in older eyes.[21,27] This spherical aberration was also introduced by using a combination of phase plates and the deformable mirror. All other higher-order wave-front aberrations present in the subjects' eyes remained unmodified.

In both cases, astigmatism was corrected by using the membrane mirror, and the subjective best-focus position was determined by allowing the subject to move the optometer (in 0.1-D steps) until a target letter E was judged to be in focus (the subjective best-focus position was determined separately for both cases). This location is referred to as the 0-D position on all figures appearing in this article. All defocused measurements were performed by defocusing the system by the desired amount relative to this best-focus position (for both cases).

In all four subjects the difference in spherical aberration between cases 1 and 2 was approximately the same. The adaptive optics vision simulator provided a reliable control to maintain this difference throughout the experiment. For both cases 1 and 2, the effect of defocus on subjective visual performance was also investigated. Contrast sensitivity (at 6 cyc/deg) and visual acuity were measured at four different defocus positions, ± 0.5 and ± 1.0 D (achieved by moving the motorized optometer). At each focus position, including best focus, the ocular wave-front aberration was measured.

Visual Acuity Testing

To determine visual acuity experimentally, subjects were asked to perform a four-alternative, forced-choice illiterate E test. The subject identified the orientation (facing left, right, up or down) of a 100% contrast letter presented for 300 ms on the high-resolution monitor of the AOVS. Five letter sizes were presented randomly, and each size was repeated 12 times. Using a nonlinear fit, these data were then applied to a Boltzman growth sigmoidal psychometric function, and the letter acuity was determined to be the stroke thickness of the letter size where 75% of the responses were correct. This procedure was performed using both green and white light and was repeated three times

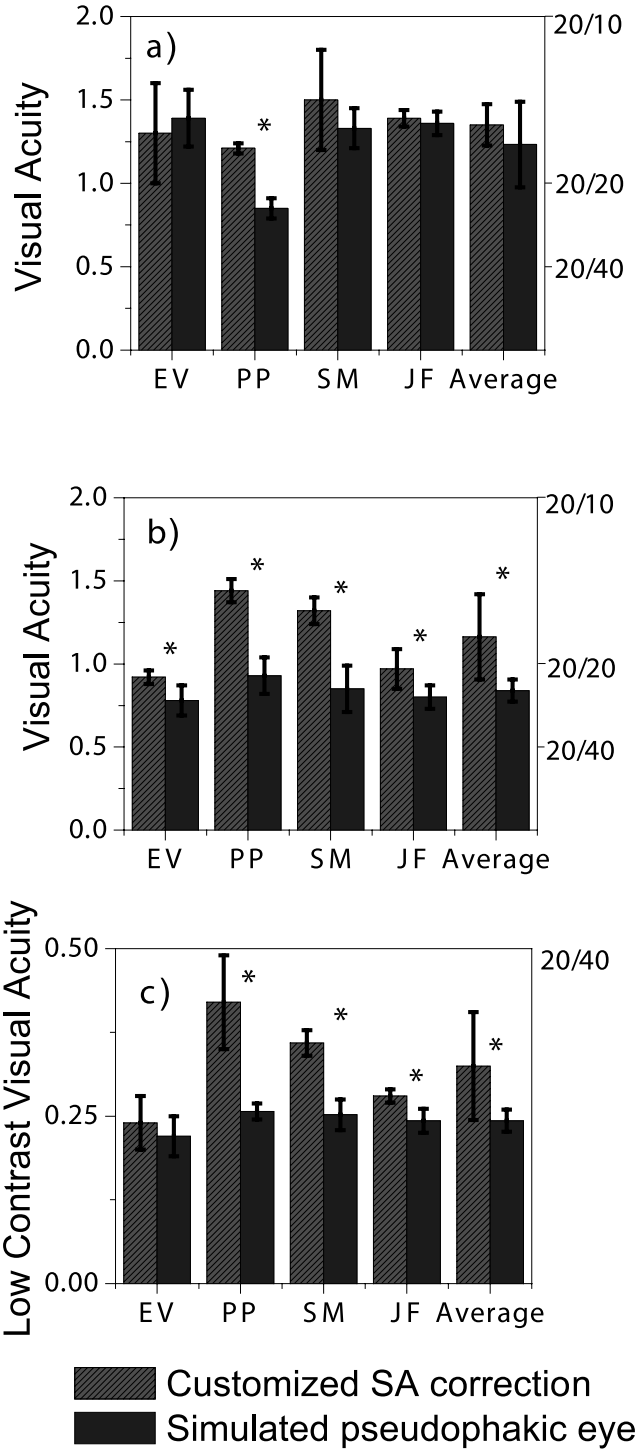

FIGURE 3. (**a**) High-contrast letter acuity measured in white light for the best-focus position (4.8-mm pupil) with spherical aberration corrected (case 1) and with 0.149 μm of spherical aberration introduced (case 2). (**b**) High-contrast letter acuity measured in green light for the best-focus position (4.8-mm pupil) for cases 1 and 2. (**c**) Low-contrast letter acuity measured in green light for the best-focus position (4.8-mm pupil) for cases 1 and 2. Note that in (**c**) the scale for visual acuity is different. *Case 1 has a statistically significantly better average acuity than case 2; $P < 0.05$.

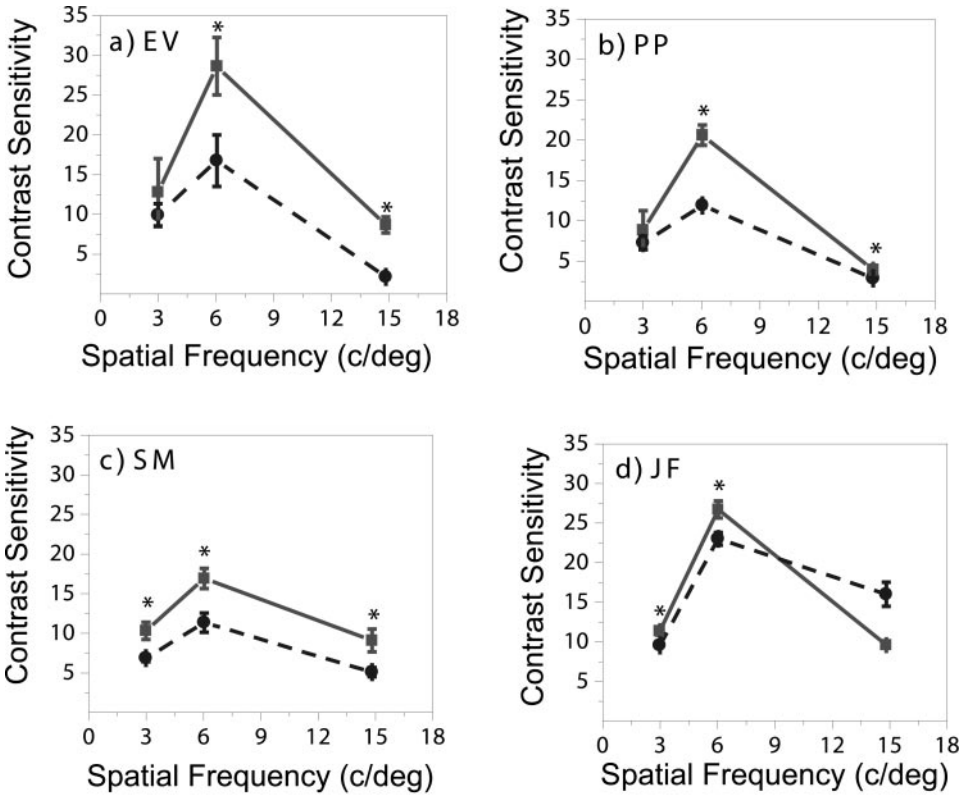

FIGURE 4. Contrast sensitivity measured in white light for a 4.8-mm pupil in the best-focus position with spherical aberration corrected (*squares*, case 1) and with 0.149 μm of spherical aberration introduced (*circles*, case 2) in subjects (**a**) EV, (**b**) PP, (**c**) SM, and (**d**) JF. *Case 1 has a statistically significantly better average contrast sensitivity than case 2; $P < 0.05$.

for the best-focus position and two times for each defocused position. Low-contrast visual acuity (LCVA) was measured with the same setup and procedure for letters with 10% contrast. LCVA was measured only in green light.

Contrast Sensitivity Measurements

Contrast thresholds were determined for three spatial frequencies (3, 6, and 15 cyc/deg) using a two-alternative, forced-choice method and

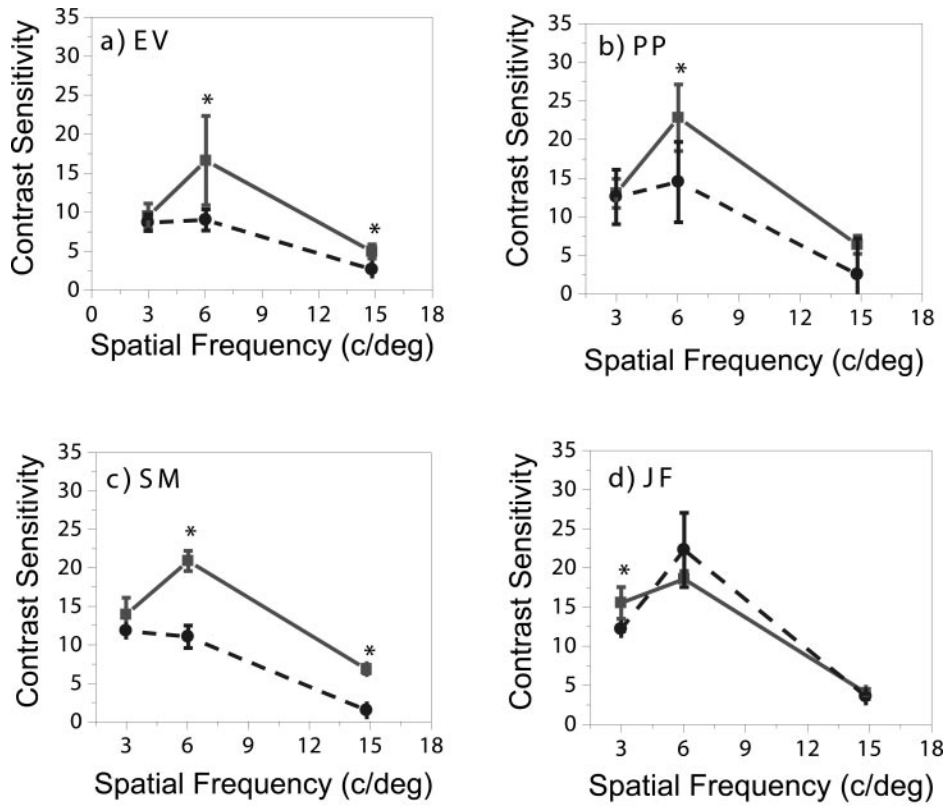

FIGURE 5. Contrast sensitivity measured in green light for a 4.8-mm pupil in the best-focus position with spherical aberration corrected (*squares*, case 1) and with 0.149 μm of spherical aberration introduced (*circles*, case 2) in subjects (**a**) EV, (**b**) PP, (**c**) SM, and (**d**) JF. *Case 1 has a statistically significantly better average contrast sensitivity than case 2, $P < 0.05$.

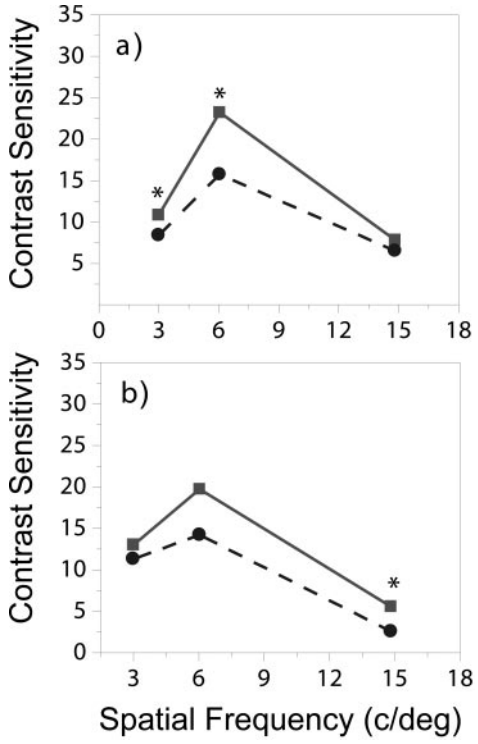

FIGURE 6. The average contrast sensitivity measured in four subjects for a 4.8-mm pupil in the best-focus position with spherical aberration corrected (*squares*, case 1) and with 0.149 μm of spherical aberration introduced (*circles*, case 2) in (**a**) white light or (**b**) green light.

the QUEST search procedure.[28] Subjects were presented with two images, one after the other, for a duration of 300 ms. A sine wave grating in a flat-topped Gaussian envelope subtending 24 minutes of arc was displayed in one of these images, and the subject was asked to determine which one. The grating image was randomly presented in one of four different orientations (−45°, 0°, 45°, and 90°) to minimize orientation effects.

This procedure was performed in the best-focus position in both green and white light and was repeated three times for each spatial frequency. For defocused positions, measurements of the contrast threshold at 6 cyc/deg were taken in green light only, and each measurement was repeated twice.

Theoretical Optical Calculations

The wave-front aberration measurements recorded for each subject at each focus position during the subjective tests were used to compute the point spread function (PSF) and the two-dimensional monochromatic modulation transfer function (MTF). The one-dimensional MTF was then calculated from the radial projection (averaged over all angles) of the two-dimensional MTF.

RESULTS

Figure 2 shows, as an example, the wave-front aberration in the best-focus position of one of the subjects (EV) with spherical aberration corrected (case 1) and with spherical aberration introduced (case 2). This subject's corresponding PSFs and MTFs are also shown. In case 1 the spherical aberration of the subject was corrected with aspheric phase plates and the membrane mirror. The average remaining spherical aberration coefficient ($Z(4,0)$), measured with the Hartmann-Shack wave-front sensor in all four subjects, was 0.001 μm for a 4.8-mm pupil. In case 2, spherical aberration was introduced (the target value was an amount similar to the average measured in pseudophakic eyes implanted with lenses with spherical surfaces), again using appropriate aspheric phase plates and the deformable mirror. In this case, the average spherical aberration coefficient ($Z(4,0)$), measured with the Hartmann-Shack wave-front sensor for the four subjects, was 0.154 μm for a 4.8-mm pupil. We measured spherical aberration in all the subjects throughout the experiment to control the stability of the mean values. Table 1 shows an example of the average spherical aberration and the SD obtained from this series of measurements. The data clearly indicate that, in the conditions of the experiment, spherical aberration was stable around the target values required. In case 1 (corrected spherical aberration) all subjects had an absolute value of spherical aberration below 0.01 μm with an SD lower than 0.02 μm. In case 2, (introduced spherical aberration) a similar range in measured spherical aberrations was recorded. From these data, we conclude that the spherical aberration was adequately controlled throughout the duration of the experiment.

Figure 3a shows the high-contrast visual acuity for the best-focus position in cases 1 and 2 measured in white light, whereas Figure 3b plots the same type of visual acuity measurements obtained in green light. Figure 3c plots the LCVA measured for cases 1 and 2 in green light. The individual LCVA for each subject is shown, in addition to the average for all four subjects. In all cases except one, the measured visual acuity was better when the spherical aberration was corrected (case 1) than when spherical aberration was introduced (case 2). The statistical significance of these improvements was investigated with a one-sided *t*-test (*$P < 0.05$; Fig. 3).

Figure 4 shows the best-focus contrast sensitivity functions (CSFs) measured in white light in all four subjects with spherical aberration corrected (squares) and introduced (circles). Contrast sensitivity is higher in all four subjects at all spatial frequencies (except JF at 15 cyc/deg) when spherical aberration is corrected. Figure 5 shows the same contrast sensitivity data measured in green light. Again, contrast sensitivity was higher in all subjects at all spatial frequencies (except JF at 6 cyc/deg) when spherical aberration was corrected. On average, the improvement in white light (Fig. 6a) is 29%, 47%, and 20% at 3, 6, and 15 cyc/deg, respectively, and in green light (Fig. 6b) is 15%, 39%, and 116% at 3, 6, and 15 cyc/deg, respectively. The statistical significance of these improvements was again investigated using a one-sided *t*-test. Statistically significant differences ($P < 0.05$) are indicated in Figures 4, 5, and 6 with an asterisk.

All results presented thus far were subjective measurements of visual performance in the best-focus position. However, we also performed visual measurements for different values of defocus around the best-focus position. Figure 7 shows as an example the wave-front aberrations and the associated PSFs for one of the subjects (EV) at the five different positions of focus without (case 1) and with (case 2) spherical aberration. Figure 8a shows the average visual acuity measured in the four subjects in white light as a function of defocus from −1D to +1D, and Figure 8b shows the same measurements taken in green light. Figure 9 shows the average contrast sensitivity at 6 cyc/deg measured in the four subjects (green light), as a function of defocus. Negative values of defocus mean a need for negatively powered spherical correction (myopia), whereas positive values refer to a need for positively powered spherical correction (hyperopia). These results suggest that, in terms of visual performance, vision is as good or better when the spherical aberration is corrected for defocus as large as 1 D. Because not all higher-order aberrations were corrected (e.g., coma and trefoil remained), each individual had a different tolerance of defocus. They also experienced a different tolerance of positive and negative defocus. Experiments performed in white light better portray the potential benefits of IOLs. As ex-

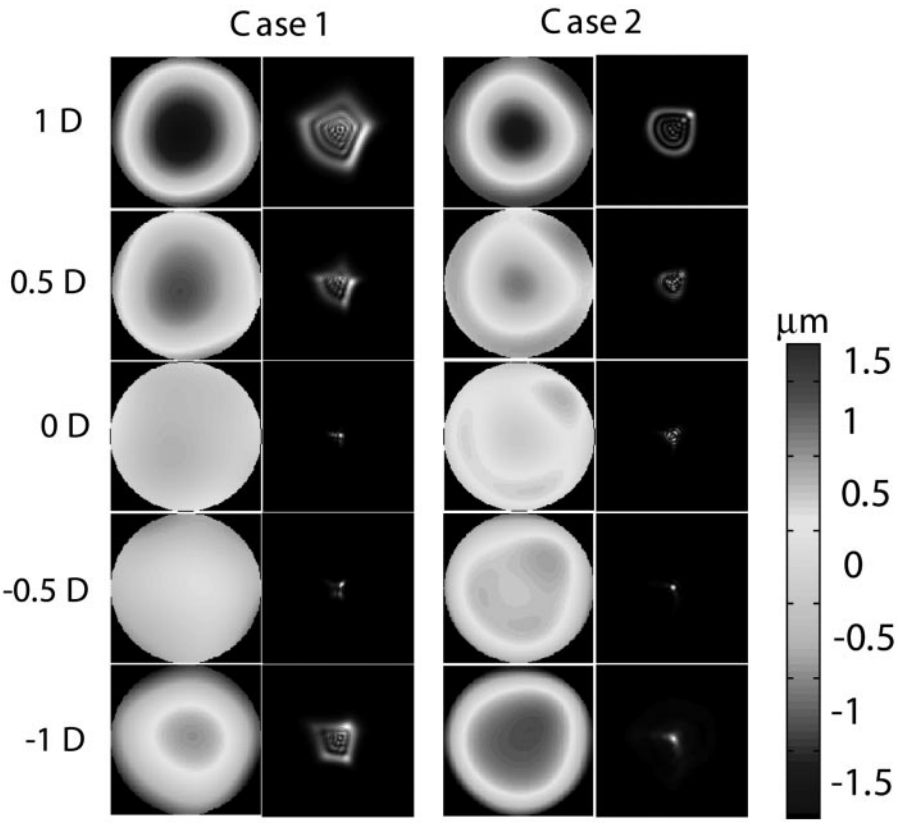

FIGURE 7. Wave-front aberrations and associated PSFs for one of the subjects (EV) at different defocus for the two cases of the study: without (case 1) and with (case 2) induced spherical aberration. Bar: in micrometers the color code for the wave-fronts.

pected,[29] defocus is more tolerable in white light than in green light when spherical aberration is corrected (relative to when spherical aberration is introduced). Also, a subject's tolerance to defocus is dependent on the target type (letters versus gratings). This is most likely because of the different spatial frequency content associated with the targets used in these two tests and the fact that as spatial frequency increases, our depth of focus decreases.[29]

The average monochromatic MTFs calculated from the wave-front aberration profiles recorded in the best-focus position for cases 1 and 2 are shown in Figure 10a. On average the contrast improvement predicted from the MTF calculations is 5%, 14%, and 106% at 3, 6, and 15 cyc/deg. The through-focus monochromatic MTFs at 6 cyc/deg for cases 1 and 2, calculated from the wave-front aberration profiles recorded during the subjective visual quality measurements, are shown in Figure 10b. These MTF calculations predict the general behavior of the visual-testing results.

DISCUSSION

A large variability exists in the ocular wave-front aberrations in different normal subjects.[30] In particular, spherical aberration is small in normal young subjects and becomes larger and positive with age,[31] with individual variation. Some people should therefore experience more improvement in visual performance than others when spherical aberration is corrected. In all four subjects assessed in this study, the simulated implantation of a customized spherical aberration–correcting IOL improved visual performance when compared with the simulated implantation of a spherically surfaced IOL. In a realistic comparison, when investigating the benefit provided to a group of patients by lenses that provide customized correction of spherical aberration, compared with a population conventional spherical lens implants, we should consider that in the spherical case (case 2), there would be a spread in the postoperative ocular spherical aberration values. In this study, we consider only the average difference, and, as such, the conclusions are valid only for this average situation. Performing measurements in a simulator allows you to determine the theoretical maximum benefits. As such, in a clinical situation, we expect the benefit of customized correction of spherical aberration to be less than what has been measured in this experiment.

As only four subjects were assessed, each of which was relatively young, with low degrees of refractive error, generalizations cannot be made to all patients with cataract. Young subjects were used in this experiment due to the desire to collect reliable psychophysical data, but the improvements presented here may not be representative of the improvements attainable in older subjects because of possible differences in modulation threshold functions (retinal contrast transfer abilities). The larger amount of aberrations in the eyes of older subjects,[31–32] compared with younger subjects may also influence the visual improvements attainable in older and younger subjects. Despite these limitations, the results obtained in this study can be compared with already published clinical results obtained with the Tecnis lens.

In the clinical study performed by Mester et al.,[8] the average difference in spherical aberration was the same as occurred in the current study in individual subjects. The average improvement in photopic contrast sensitivity measured using a Functional Acuity Contrast Chart (FACT chart; Vision Sciences Research Corp., San Ramon, CA) at 6 cyc/deg was 30% as opposed to the 47% measured in this study (for the white light condition). This relative increase in visual performance can be explained by a number of factors. First, in this study, all subjects had customized correction of their individual spherical aberration, whereas in the Mester et al. study all patients received an average correction. The luminance conditions and

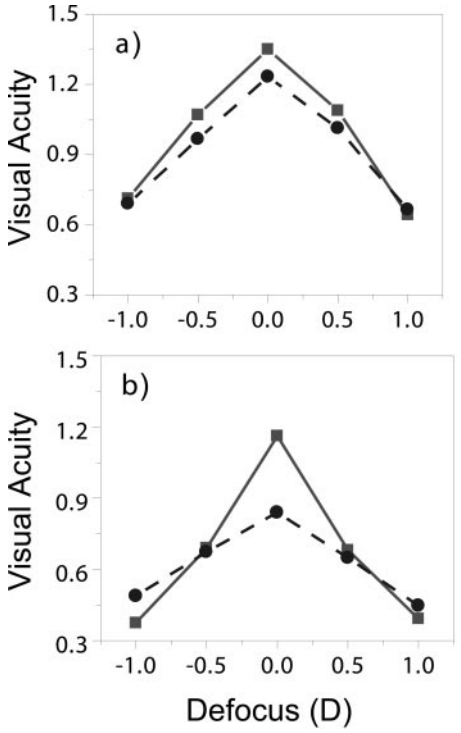

FIGURE 8. The average through-focus visual acuity measured for a 4.8-mm pupil with spherical aberration corrected (*squares*, case 1) and with 0.149 μm of spherical aberration introduced (*circles*, case 2) in (**a**) white light or (**b**) green light.

pupil sizes were also different in the two studies. In the clinical study by Mester et al. the photopic contrast sensitivity was measured at 85 while 35 cd/m^2 was used in this study. In addition, the pupil size of the patients with cataract was controlled by the ambient lighting conditions and was therefore a natural pupil size, whereas in the simulator the pupils of all subjects were pharmacologically dilated and an artificial pupil size was imposed (4.8 mm). This most likely played a role in the fact that the contrast sensitivity values measured in this study were lower than values that are typically measured in a clinical setting for contrast sensitivity. These low values can also be explained by the fact that, although the luminance conditions were photopic, they were on the low end of the photopic scale, and the pupil sizes were relatively large for photopic conditions. In addition, although patients are given no time restrictions on identifying a target in clinical measurements of contrast sensitivity (using a contrast sensitivity chart), the identification task performed on the simulator is made more difficult by the fact that subjects are presented with the target for only 0.3 seconds.

The different levels of improvement measured for different psychophysical tests administered during this study draws attention to the fact that the potential benefit derived from improvements in the visual system varies, depending on the target chosen for the assessment. In white light the average improvement in visual acuity associated with customized correction of spherical aberration was 10%, whereas for the same conditions, the average improvement in the CSF was 32% (as an average of the three spatial frequencies). Similarly, in green light, the average improvement in visual acuity associated with customized correction of spherical aberration was 38%, whereas, for the same conditions, the average improvement in the CSF was 57% (again as an average of the three spatial frequencies). This reflects the fact that contrast sensitivity testing is more sensitive to changes in the retinal contrast than is visual acuity testing.[33] Also, retinal images of contrast sensitivity targets contain one pure spatial frequency (even for a defocused eye), whereas high-contrast letters are complex targets that contain more than one spatial frequency. As a result, retinal images of defocused letters may contain phase-contrast reversals. In fact, one subject commented that phase-contrast reversals under defocused conditions made it easier to identify letter orientation. In other studies of the potential of customized wave-front aberration correction,[4,7] higher spatial frequencies were chosen for subjective performance tests, because theoretical optical calculations of the MTF reveal that higher spatial frequencies have more potential for improvement. However, we chose to use lower spatial frequencies or the areas around the peak of the CSF curve, because these peak frequencies are more closely correlated with functional vision.[34] In a normal population, this peak often occurs at ~6 cyc/deg,[35] whereas recent studies of the contrast sensitivities of pseudophakic individuals reveal that their peak is ~3 cyc/deg.[8,19,20]

It is not surprising that correcting spherical aberration provides a visual benefit.[36] From the results obtained in this study, it seems clear that there are potential benefits to customized correction of spherical aberration in cataract patients who use IOLs. Naturally, patients who have large amounts of spherical aberration, either due to normal aging or to LASIK for myopia correction[6] (in this case, LASIK that does not provide wave-front correction) would benefit more from customized correction. Correction with an IOL is sensitive to tilt and decentration of the IOL. Bench measurements of the Tecnis lens indicate that if it is decentered 0.5 mm and tilted <7°. Its optical performance will exceed that of a conventional spherical IOL.[21] A higher level of spherical aberration correction would be even more sensitive to correct placement in the eye. The potential benefits associated with the customized correction of spherical aberration are reduced when the pupil is small. As a result, the improvement in visual performance would be largest in younger patients where the pupil is large or in situations where the pupil is dilated due to low light conditions such as driving at night. Yoon and Williams[7] revealed that there are large visual benefits associated with the correction of all monochromatic higher-order wave-front aberrations. A study of whether the correction of the remaining higher-order aberrations is practical and realizable using customized IOLs should be performed. The effect of the correction of all these aberrations on depth of focus should also be investigated.

In this study, through-focus measurements of visual performance were conducted to achieve a better understanding of the impact of spherical aberration on pseudoaccommodation

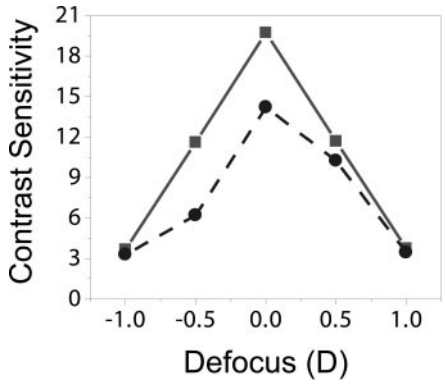

FIGURE 9. The average through-focus contrast sensitivity at 6 cyc/deg measured for a 4.8-mm pupil with spherical aberration corrected (*squares*, case 1) and with 0.149 μm of spherical aberration introduced (*circles*, case 2) in green light.

due to depth of focus. The classic definition of depth of focus is the range of defocus values for which there is a blur of small enough size that it will not adversely affect the performance of the system. Thus, when the MTF is used for assessment the 80% criterion is often used to determine depth of focus, which is the defocus range over which the MTF is greater than 80% of the peak MTF.[29] Figure 11 illustrates the application of this criterion to model eyes with spherical aberrations that are the same as in cases 1 and 2 in the experiments conducted in this study. Using the MTF of idealistic on-axis eye models (containing no higher-order aberrations other than spherical aberration) and the 80% criterion, depth of focus is increased by adding spherical aberration to the eye model. Similar behavior is observed in the measurements. If the 80% criterion is applied to the contrast sensitivity data collected in the AOVS (Fig. 9), depth of focus with spherical aberration corrected (case 1) again is less than depth of focus with spherical aberration introduced (case 2). As a result, we see that this definition of depth of focus may not be the most relevant definition when functional vision is considered. Indeed, with spherical aberration correction our results suggest that the range of functional vision is not decreased and that the average visual performance is as good or better when spherical aberration is corrected for as much as 1 D of defocus. This may be because even in the corrected state other higher order aberrations remain (average RMS error was still 0.25 μm after correcting the spherical aberration). This serves to flatten the MTF versus defocus curves shown in Figure 11 so that they appear more like those in Figure 10b and allow the subjects to have more tolerance to defocus. The 80% criterion is an arbitrary criterion that may not

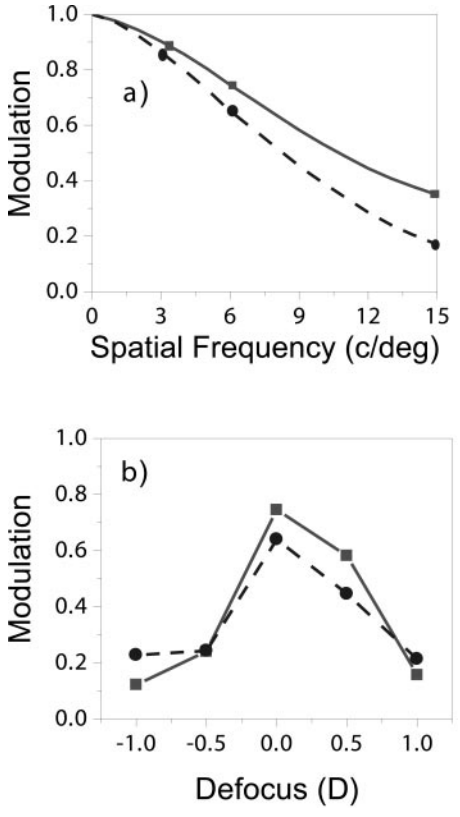

FIGURE 10. (**a**) Average monochromatic MTFs calculated from the measured wave-front aberration profiles for a 4.8-mm pupil in the best-focus position with spherical aberration corrected (*squares*, case 1) and with 0.149 μm of spherical aberration introduced (*circles*, case 2). (**b**) The average through-focus contrast sensitivity at 6 cyc/deg measured in green light for a 4.8-mm pupil for the two cases.

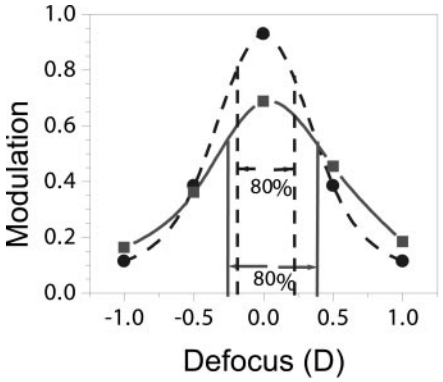

FIGURE 11. Theoretical through-focus MTF calculated using on-axis eye models (4.8-mm pupil and 6 cyc/deg) where the only aberration present is spherical aberration for cases 1 (*circles*) and 2 (*squares*).

reflect the nature of tolerance to defocus in the visual system. It may be more relevant to use an absolute threshold metric that is individually determined. More investigation is needed to determine a functional definition of the subjective depth of focus.

Using monochromatic eye models and the recorded wave-front aberration, we calculated the MTF and used it to predict the improvements possible (Fig. 10). These predictions were then compared with the measured monochromatic contrast sensitivity outcomes (Figs. 6b, 9). In general, there is a reasonable qualitative agreement between the optical (MTF) and visual parameters (CSF) studied in agreement with previous studies of this issue.[37] Quantitatively, the improvement measured when spherical aberration is corrected is underestimated by the predictions provided by the theoretical optical calculations (especially when the eye is defocused). This may be explained by the Stiles-Crawford effect, which was not included in the eye model and which may affect the optical predictions and the psychophysical measurements differently. However, for the pupil size studied (4.8 mm), it is assumed that the Stiles-Crawford effect plays a relatively minor role[38] and does not explain the differences between the two assessment techniques. Because eye models do not always provide us with a complete description of the potential improvements in visual performance associated with new optical innovations, adaptive optics simulators have become useful tools.

Through the use of adaptive optics it is possible to correct precisely the higher-order wave-front aberrations of the eye. Although this technique can only be used in laboratory simulations with complicated and expensive equipment, it provides us with a noninvasive method for exploring the potential of new ophthalmic devices. Adaptive optics also provides us with a powerful tool for the interactive design of new ophthalmic devices and a way to test the relationship between ocular optical quality and visual performance under different conditions.

References

1. Liang J, Williams DR. Aberrations and retinal image quality of the normal human eye. *J Opt Soc Am A*. 1997;14:2873–2883.
2. Artal P, Guirao A, Berrio E, Williams DR. Compensation of corneal aberrations by the internal optics in the human eye. *J Vision*. 2001;1:1–8.
3. Tang CY, Charman WN. Effects of monochromatic and chromatic oblique aberrations on visual performance during spectacle lens wear. *Ophthalmic Physiol Opt*. 1992;12:340–349.
4. Liang J, Williams DR, Miller DT. Supernormal vision and high-resolution retinal imaging through adaptive optics. *J Opt Soc Am A*. 1997;14:2884–2892.

5. Seiler T, Mrochen M, Kaemmerer M. Operative correction of ocular aberrations to improve visual acuity. *J Refract Surg*. 2000;16: S619–S622.
6. Marcos S. Aberrations and visual performance following standard laser vision correction. *J Refract Surg*. 2001;17:S596–S601.
7. Yoon GY, Williams DR. Visual performance after correcting the monochromatic and chromatic aberrations of the eye. *J Opt Soc Am A*. 2002;19:266–275.
8. Mester U, Dillinger P, Anterist N. Impact of a modified optic design on visual function: clinical comparative study. *J Cataract Refract Surg*. 2003;29:652–660.
9. Guirao A, Porter J, Williams DR, Cox IG. Calculated impact of higher-order monochromatic aberrations on retinal image quality in a population of human eyes. *J Opt Soc Am A*. 2002;19:1–9.
10. Vargas-Martin F, Prieto PM, Artal P. Correction of the aberrations in the human eye with a liquid-crystal spatial light modulator: limits to performance. *J Opt Soc Am A*. 1998;15:2552–2562.
11. Fernandez EJ, Iglesias I, Artal P. Closed-loop adaptive optics in the human eye. *Opt Lett*. 2001;26:746–748.
12. Hofer H, Chen L, Yoon GY, Singer B, Yamauchi Y, Williams DR. Improvement in retinal image quality with dynamic correction of the eye's aberrations. *Opt Express*. 2001;8:631–643.
13. Fernandez EJ, Manzanera S, Piers P, Artal P. Adaptive optics visual simulator. *J Refract Surg*. 2002;18:S634–S638.
14. Navarro R, Moreno-Barriuso E, Bara S, Mancebo T. Phase plates for wave-aberration compensation in the human eye. *Opt Lett*. 2000; 25:236–238.
15. Mrochen M, Kaemmerer M, Seiler T. Clinical results of wavefront-guided laser in situ keratomileusis 3 months after surgery. *J Cataract Refract Surg*. 2001;27:201–207.
16. Sarkisian KA, Petrov AA. Clinical experience with the customized low spherical aberration ablation profile for myopia. *J Refract Surg*. 2002;18:S352–S356.
17. Lopez-Gil N, Castejon-Mochon JF, Benito A, et al. Aberration generation by contact lenses with aspheric and asymmetric surfaces. *J Refract Surg*. 2002;18:S603–S609.
18. Guirao A, Redondo M, Geraghty E, Piers P, Norrby S, Artal P. Corneal optical aberrations and retinal image quality in patients in whom monofocal intraocular lenses were implanted. *Arch Ophthalmol*. 2002;120:1143–1151.
19. Kershner RM. Retinal image contrast and functional visual performance with aspheric, silicone, and acrylic intraocular lenses: prospective evaluation. *J Cataract Refract Surg*. 2003;29:1684–1694.
20. Packer M, Fine IH, Hoffman RS, Piers P. Prospective randomized trial of an anterior surface modified prolate intraocular lens. *J Refract Surg*. 2002;18:692–696.
21. Holladay JT, Piers PA, Koranyi G, van der Mooren M, Norrby NE. A new intraocular lens design to reduce spherical aberration of pseudophakic eyes. *J Refract Surg*. 2002;18:683–691.
22. Campbell FW. The depth of field of the human eye. *Opt Acta*. 1957;4:157–164.
23. Nio YK, Jansonius NM, Fidler V, Geraghty E, Norrby S, Kooijman AC. Spherical and irregular aberrations are important for the optimal performance of the human eye. *Ophthalmic Physiol Opt*. 2002;22:103–112.
24. Fernandez EJ, Artal P. Membrane deformable mirror for adaptive optics: performance limits in visual optics. *Opt Express*. 2003;11: 1056–1069.
25. Prieto PM, Vargas-Martin F, Goelz S, Artal P. Analysis of the performance of the Hartmann-Shack sensor in the human eye. *J Opt Soc Am A*. 2000;17:1388–1398.
26. Vdovin G, Sarro PM. Flexible mirror micromachined in silicon. *Appl Opt*. 1995;34:2968–2972.
27. Guirao A, Redondo M, Artal P. Optical aberrations of the human cornea as a function of age. *J Opt Soc Am A*. 2000;17:1697–1702.
28. Watson AB, Pelli DG. QUEST: a Bayesian adaptive psychometric method. *Percept Psychophys*. 1983;33:113–120.
29. Marcos S, Moreno E, Navarro R. The depth-of-field of the human eye from objective and subjective measurements. *Vision Res*. 1999;39:2039–2049.
30. Porter J, Guirao A, Cox IG, Williams DR. Monochromatic aberrations of the human eye in a large population. *J Opt Soc Am A*. 2001;18:1793–1803.
31. Artal P, Berrio E, Guirao A, Piers P. Contribution of the cornea and internal surfaces to the change of ocular aberrations with age. *J Opt Soc Am A*. 2002;19:137–143.
32. McLellan JS, Marcos S, Burns SA. Age-related changes in monochromatic wave aberrations of the human eye. *Invest Ophthalmol Vis Sci*. 2001;42:1390–1395.
33. Williams DR, Yoon GY, Guirao A, Hofer H, Porter J. How far can we extend the limits of human vision. In: MacRae SM, Kreuger RR, Applegate RA, eds. *Customized Corneal Ablation: The Quest for Supervision.* Thorofare, NJ: Slack Inc.; 2001:11–32.
34. Ginsburg AP, Evans DW, Sekule R, Harp SA. Contrast sensitivity predicts pilots' performance in aircraft simulators. *Am J Optom Physiol Opt*. 1982;59:105–109.
35. Nio YK, Jansonius NM, Fidler V, Geraghty E, Norrby S, Kooijman AC. Age-related changes of defocus-specific contrast sensitivity in healthy subjects. *Ophthalmic Physiol Opt*. 2000;20:323–334.
36. Applegate RA, Sarver EJ, Khemsara V. Are all aberrations equal? *J Refract Surg*. 2002;18:S556–S562.
37. Villegas EA, Gonzalez C, Bourdoncle B, Bonnin T, Artal P. Correlation between optical and psychophysical parameters as a function of defocus. *Optom Vis Sci*. 2002;79:60–67.
38. Atchison DA, Scott DH, Strang NC, Artal P. Influence of Stiles-Crawford apodization on visual acuity. *J Opt Soc Am A*. 2002;19: 1073–1083.